

# Improved Method for Determining the $n$ -Value of HTS Bulks

Bruno Douine, Kévin Berger, Charles-Henri Bonnard, *Student Member, IEEE*,  
Frédéric Sirois, *Senior Member, IEEE*, Abelin Kameni Ntichi, and Jean Lévêque.

**Abstract**— The complete penetration magnetic field  $B_P$  is the main feature of a superconducting pellet submitted to an axial applied magnetic field. The electric  $E$ - $J$  characteristics of HTS bulk is generally described by a power law  $E(J) = E_C(J/J_C)^n$ . The influence of the  $n$ -value and applied magnetic field rise rate  $V_b$  on the  $B_P$  of a HTS cylindrical pellet has been presented in a previous paper. The numerical results presented come from numerical resolution of a non linear diffusion problem. With the help of these simulations a linear relationship between  $B_P$ ,  $\ln V_b$  and  $n$ -value has been deduced. This comparison allows determining the critical current density  $J_C$  and the  $n$ -value of the power law based on direct measurement of  $B_P$  in the gap between two bulk HTS pellets. In this paper, an improvement of this method is presented. The influence of geometric parameters  $R$  and  $L$  is studied to give generality to the relationship between  $B_P$ ,  $V_b$  and  $n$ -value. Previous  $B_P$  formula is confirmed by these new simulations. To correctly connect simulation and experimental results, the influence of spacing  $e$  between bulks is studied and presented. A relationship between  $B_P$  and measured complete penetration magnetic field  $B_{PM}$  is determined.

**Index Terms**—Critical current density, magnetic field diffusion, superconductors.

## I. INTRODUCTION

THE use of high temperature superconductor (HTS) bulks for electric motors, generators or magnetic levitation systems is now feasible due to high critical current density and progress of cryogenics [1]–[7]. For low temperature superconductors (LTS) or HTS materials used at low temperatures, the critical state model (CSM) is used [8]. Since in the CSM  $J$  can only take well defined values such as 0 or  $J_C$  (critical current density) that do not depend on the rate of variation of the externally applied field. Because of this simple relationship,  $J_C$  can be determined by magnetization experiments [9], [10].

If a cylindrical HTS pellet is submitted to an uniform axial applied magnetic field  $B_a(t)$  as in Fig. 1, the magnetic field at the center of the pellet  $B_0(t)$  starts to rise after some time delay  $T_p$ , related to the moment at which  $B_a$  reaches  $B_P$ , Fig. 2. For cylinders, and assuming CSM applies, an analytic expression

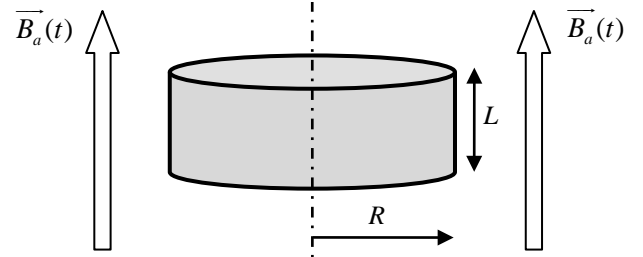


Fig. 1. Bulk superconducting pellet of cylindrical shape submitted to a uniform axial magnetic field.

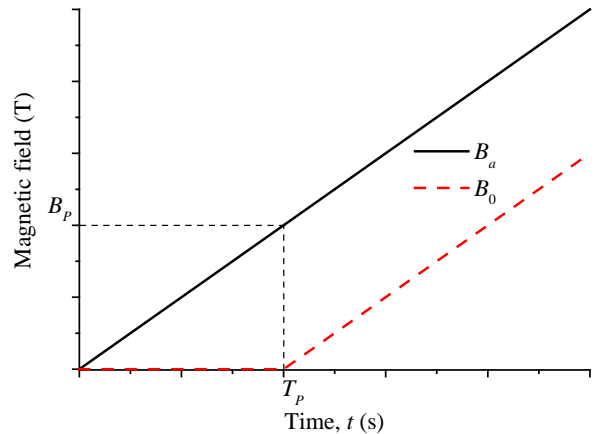


Fig. 2. Linear growth of the applied magnetic field  $B_a$  and the theoretical magnetic field  $B_0$  at the center of the pellet versus time  $t$ .

for the complete penetration field, named  $B_{PB}$ , can be obtained based on the application of the Biot–Savart law [10]–[12]:

$$B_{PB} = \frac{\mu_0 J_C L}{4} \ln \left( \frac{\sqrt{R^2 + \left(\frac{L}{2}\right)^2} + R}{\sqrt{R^2 + \left(\frac{L}{2}\right)^2} - R} \right) \quad (1)$$

where  $L$  is the length of cylinder and  $R$  is its radius.

In the case of HTS used at “high temperatures”, typically above 50-60 K, a power law model better represents the  $E(J)$  characteristic of the materials than the CSM model [11]–[17]. The power law model is typically written as:

$$E = E_C \left( \frac{J}{J_C} \right)^n = \frac{E_C}{J_C} \left( \frac{J}{J_C} \right)^{n-1} J \quad (2)$$

The critical current density  $J_C$  and the  $n$ -value depend on temperature, magnetic field and there is an inhomogeneity of  $J_C$  over the volume [14]. However, in this paper  $J_C$  and  $n$ -

B. Douine, K. Berger, C.H. Bonnard and J. Lévêque with the University of Lorraine, GREEN, Research Group in Electrical engineering and Electronics of Nancy - EA 4366, Faculté des Sciences et Technologies, BP 70239, 54506 Vandoeuvre-lès-Nancy Cedex, France (e-mail: name.surname@univ-lorraine.fr).

F. Sirois is with Ecole Polytechnique of Montreal, Montreal, QC H3C3A7, Canada (e-mail: f.sirois@polymtl.ca)

A. Kameni is with Group of Electrical Engineering of Paris (GeePS), Gif-sur-Yvette, France (e-mail: abelin.kameni@supelec.fr).

value are assumed constant. The determination of the  $J_C$  and  $n$  parameters defining the power law model for a given bulk superconductor is not simple. Typical  $n$ -values vary between 10 and 50 at 77 K [18]–[20]. The calculation of the magnetization of superconducting samples assuming power law model generally requires numerical simulations. A new method of determination of  $J_C$  and  $n$ , by studying the influence of the  $n$ -value and the applied magnetic field rising rate  $V_b$  on the complete penetration magnetic field  $B_P$  is presented in [11]. For cylinders, and assuming power law model, an analytic expression for the complete penetration field, named  $B_P$ , has been deduced:

$$B_P = B_{PB} \left( 1 + \frac{\alpha \ln V_b + \beta}{n} \right) \quad (3)$$

During all the simulations, the applied magnetic field  $B_a(t)$  was a linearly increasing field, as shown in Fig. 2. The pellet has a radius  $R$  of 10 mm and a thickness  $L$  of 10 mm, which corresponds to the pellets used in the experimental part of this work. The value of  $J_C$  chosen was 100 A/mm<sup>2</sup>, which is a realistic value for HTS bulks at 77 K. For this particular case [11],  $\alpha = 1.2$  and  $\beta = 3.4$  have been deduced from simulation curves. In this paper, the influence of the geometrical parameters  $R$  and  $L$  is studied in order to give a more general formula (3).

Based on (3), the power law model parameters  $J_C$  and  $n$  of a cylindrical sample are determined from experimental measurements as described in [11]. In order to use the results derived above by simulations, one need to measure the complete penetration magnetic field  $B_P$  in the pellets. The main idea of our method is to separate the studied pellet in two pellets to allow deducing  $B_P$  from measurement of the complete penetration magnetic field  $B_{PM}$  between these two pellets. The magnetic field is detected with an axial Hall probe placed on the central axis of two HTS pellets, Fig. 3. The cylindrical HTS pellets used in this experiment were YBCO pellets with 10 mm of radius and 5 mm of thickness. In the simulation, the thickness of the corresponding pellet was taken as  $L$ , i.e. the sum of the two half-pellets. To correctly connect simulation and experimental results, the influence of the Hall probe thickness  $e$  must be taken into account. In this paper, the influence of the spacing  $e$  between the bulk pellets is presented.

## II. INFLUENCE OF CRITICAL CURRENT DENSITY AND GEOMETRIC SIZES ON $B_P$

In (3),  $B_P$  is the product of two functions. The first one is  $B_{PB}$  and the second one a function of  $V_b$  and  $n$ -value. In [11], the following assumptions are assumed:  $J_C$  and the geometric parameters  $R$  and  $L$  are only included in  $B_{PB}$  and excluded from the second one. To check these assumptions, new simulations were made with different  $J_C$  and different  $L/R$  ratios. In these simulations one HTS pellet is submitted to a linearly increasing applied magnetic field  $B_a(t)$  as shown in Fig. 2. As shown in a previous article [10], thermal effects can be neglected in our study. In these simulations chosen  $n$ -

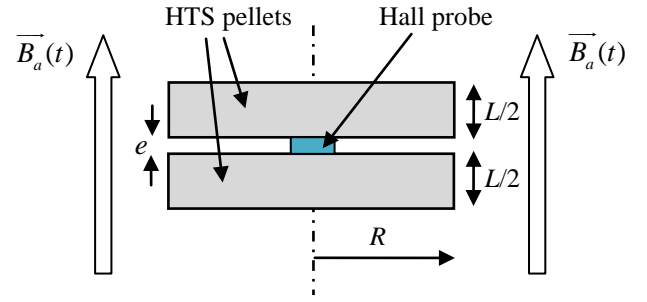


Fig. 3. Hall probe location between the two HTS pellets.

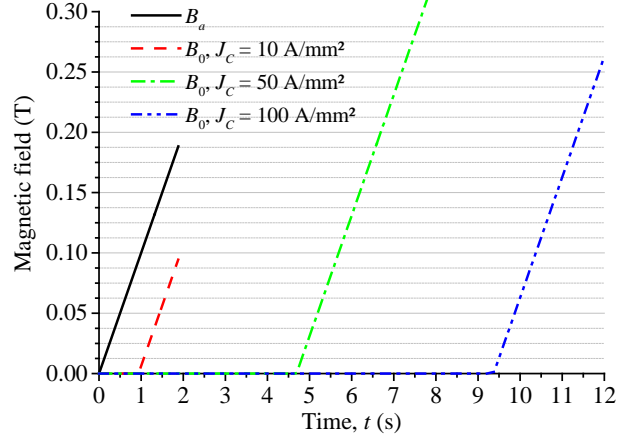


Fig. 4. Applied magnetic field and magnetic field at the center of the pellet with  $R = 10$  mm,  $L = 10$  mm,  $n = 15$ ,  $V_b = 1$  T/s and different  $J_C$ .

values are 15, 25 and 50.

### A. Simulations with different values of $J_C$

In these simulations,  $R = 10$  mm,  $L = 10$  mm,  $n = 15$ ,  $V_b = 1$  T/s, and  $B_a(t)$  and  $B_0(t)$  are represented in Fig. 4 for three different values of  $J_C$ , 10 A/mm<sup>2</sup>, 50 A/mm<sup>2</sup> and 100 A/mm<sup>2</sup>. Fig. 4 clearly shows that  $T_P$  is proportional to  $J_C$ . The same conclusion is obtained with other  $n$ -values. As  $B_P = V_b \cdot T_P$ ,  $B_P$  is also proportional to  $J_C$ .  $B_{PB}$  can also be calculated from  $B_P$  using (3) and then be compared to (1). Using (3) with  $n = 15$ , one can calculate  $B_{PB} = 0.91$  T with  $J_C = 100$  A/mm<sup>2</sup>, and  $B_{PB} = 0.091$  T with  $J_C = 10$  A/mm<sup>2</sup>. The same values of  $B_{PB}$  were obtained using (1). These results are confirmed for different rise rates from 0.01 T/s to 1000 T/s. These results prove that the assumption that  $J_C$  is included in  $B_{PB}$  is valid.

### B. Simulations with different $L/R$ ratios

In these simulations, the  $n$ -values are chosen equals to 15,  $R = 10$  mm and the  $L/R$  ratios of the pellet vary from 0.5 to 3. These values are commonly observed on commercial HTS pellets. For  $n = 15$ ,  $B_a(t)$  and  $B_0(t)$  are represented in Fig. 5 for six different values of  $L/R$  ratios. From these curves,  $B_P$  values are deduced. As expected,  $B_P$  increases with the  $L/R$  ratio at a given  $R$ . For these  $L/R$  ratios,  $B_{PB}$  is calculated from (1). Finally, the ratio  $B_P/B_{PB}$  is calculated and represented on Fig. 6. For all the rise rates and the  $n$ -values tested,  $B_P/B_{PB}$  remains constant whatever the  $L/R$  ratio. It demonstrates that the geometric parameters  $R$  and  $L$  only affect  $B_{PB}$  and not the parameters  $\alpha$  and  $\beta$  of (3).

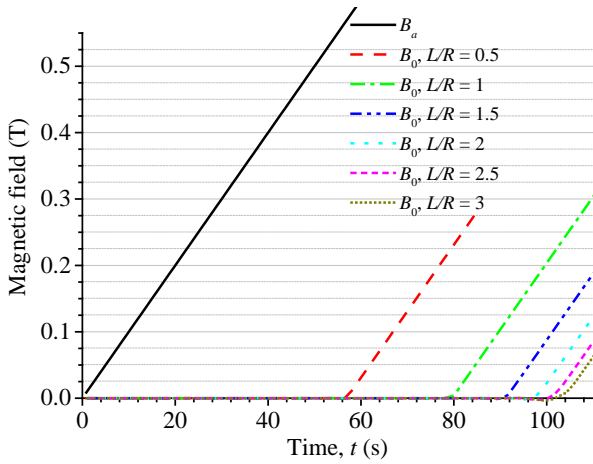


Fig. 5. Applied magnetic field and magnetic field at the center of the pellet with  $R = 10$  mm,  $n = 15$ ,  $V_b = 0.01$  T/s,  $J_C = 100$  A/mm<sup>2</sup> and different  $L/R$  ratios.

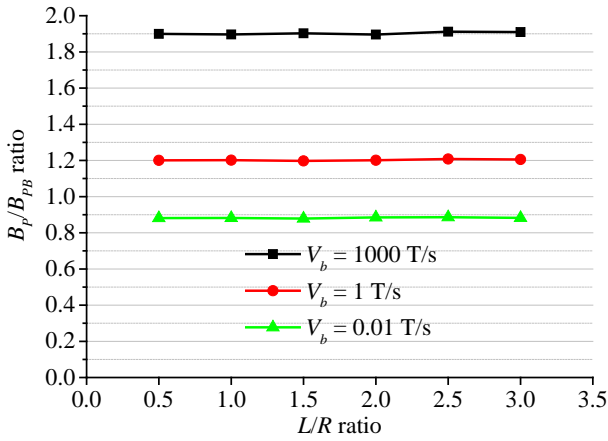


Fig. 6.  $B_p/B_{PB}$  ratio vs  $L/R$  ratio for  $n = 15$ ,  $J_C = 100$  A/mm<sup>2</sup> and different  $V_b$ .

### III. INFLUENCE OF THE SENSOR THICKNESS ON $N$ -VALUE AND $J_C$ DETERMINATION

As described in [11], experiments results give the measured complete penetration magnetic field  $B_{PM}$  and not  $B_P$ . So it is crucial to find relationship between both. In order to obtain it, simulations have been made with two HTS pellets and different spacings corresponding to the typical thicknesses of Hall probes, i.e.  $e = 0.5$  mm and 1 mm. In this paper, we called  $B_{PM}$  the measured complete penetration magnetic field obtained by simulations of realistic cases. Then, we compared the results with those of a single pellet without Hall probe, i.e.  $e = 0$  mm from which we have deduced  $B_P$ . In previous study [11], only one value of  $L$  and one value of  $V_b$  were used in simulations. In this present work, results with different  $V_b$  values and different  $L$  values are presented. This allows giving generality to this work. The applied magnetic field and the magnetic field at the center between the two pellets, with  $n = 15$ ,  $V_b = 1000$  T/s,  $J_C = 100$  A/mm<sup>2</sup>,  $R = 10$  mm,  $L = 10$  mm and different sensor thicknesses are presented in Fig. 7. As a previous study [10] showed, the shape of magnetic field at the center, between the two pellets for  $e = 0.5$  and 1 mm, is not linear around  $T_p$  even if  $B_a(t)$  is linear, Fig. 7. To allow the determination of the values of  $T_p$  for  $e = 0.5$  and 1 mm, dash lines are superimposed on  $B_0$  in

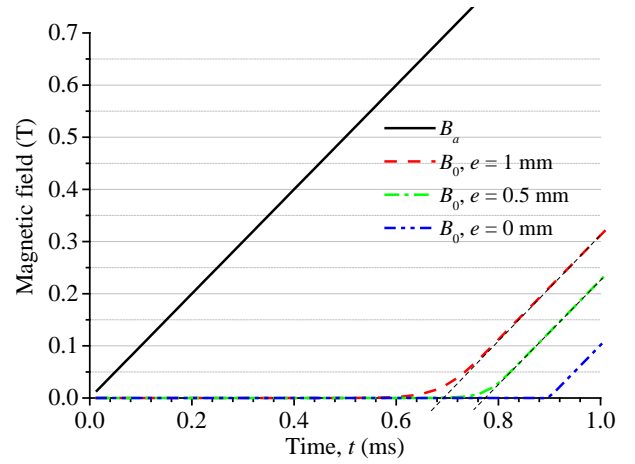


Fig. 7. Applied magnetic field and magnetic field at the center of the pellet with  $R = 10$  mm,  $n = 15$ ,  $V_b = 1000$  T/s,  $J_C = 100$  A/mm<sup>2</sup>,  $L = 10$  mm, and two different sensor thicknesses,  $e = 0.5$  and 1 mm

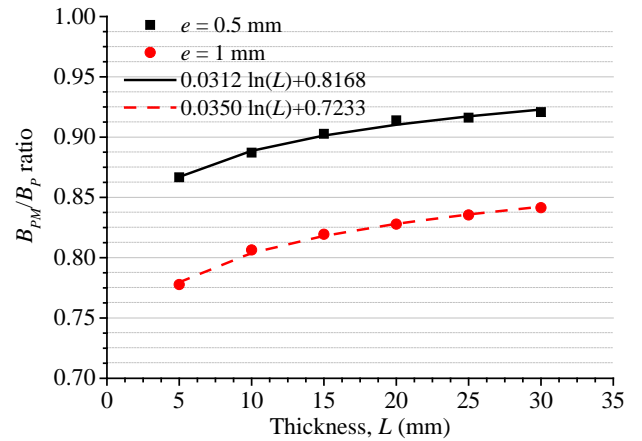


Fig. 8.  $B_{PM}/B_P$  ratio for  $e = 0.5$  and 1 mm,  $R = 10$  mm,  $n = 15$ ,  $J_C = 100$  A/mm<sup>2</sup>,  $V_b = 1000$  T/s.

Fig. 7. From these values of  $T_p$  for  $e = 0.5$  and 1 mm, values of  $B_{PM}$  are deduced. Finally  $B_{PM}/B_P$  is calculated for  $e = 0.5$  mm and 1 mm and different values of  $L$ , Fig. 8.

Two relationships between  $B_{PM}/B_P$  and  $L$  are deduced:

$$\frac{B_{PM}}{B_P}(e = 0.5 \text{ mm}) = 0.0312 \ln(L) + 0.8168, \quad (4)$$

$$\frac{B_{PM}}{B_P}(e = 1 \text{ mm}) = 0.0350 \ln(L) + 0.7233. \quad (5)$$

Equations (4) and (5) remain the same for different  $n$ -values and different values of rise rate  $V_b$ . So (4) and (5) are not dependant of  $n$  and  $V_b$ . However, (4) and (5) are available only for  $R = 10$  mm. Therefore, for each value of  $R$  new relationship between  $B_{PM}$  and  $B_P$  have to be calculated. In this work we want to show that it is possible to calculate  $B_P$  from measurement of  $B_{PM}$ . Future work has to give more general relationships between  $B_{PM}/B_P$  and geometric parameters  $e$ ,  $R$  and  $L$ .

### IV. CONCLUSION

The validity of our formula for the complete penetration magnetic field is proved and reinforced by many simulations.

The influence of sensor thickness on experimental determination of  $n$ -value is presented. Relationship between theoretical  $B_P$  and measured  $B_{PM}$  is determined. In this method, constant  $J_C$  and  $n$ -value are assumed. In future work, taking into account  $J_C(B)$  with this method may be a new goal.

## REFERENCES

- [1] A. Rezzoug, J. L ev eque, B. Douine, and S. Mezani, "Superconducting Machines," in *Non-conventional Electrical Machines*, John Wiley & Sons, Inc, 2011, pp. 191–255.
- [2] E. H. Ailam, D. Netter, J. Leveque, B. Douine, P. J. Masson, and A. Rezzoug, "Design and Testing of a Superconducting Rotating Machine," *IEEE Transactions on Applied Superconductivity*, vol. 17, no. 1, pp. 27–33, Mar. 2007.
- [3] R. Moulin, J. Leveque, L. Durantay, B. Douine, D. Netter, and A. Rezzoug, "Superconducting Multistack Inductor for Synchronous Motors Using the Diamagnetism Property of Bulk Material," *IEEE Transactions on Industrial Electronics*, vol. 57, no. 1, pp. 146–153, Jan. 2010.
- [4] P. J. Masson, M. Breschi, P. Tixador, and C. A. Luongo, "Design of HTS Axial Flux Motor for Aircraft Propulsion," *IEEE Transactions on Applied Superconductivity*, vol. 17, no. 2, pp. 1533–1536, Jun. 2007.
- [5] W. Xian, Y. Yan, W. Yuan, R. Pei, and T. A. Coombs, "Pulsed Field Magnetization of a High Temperature Superconducting Motor," *IEEE Transactions on Applied Superconductivity*, vol. 21, no. 3, pp. 1171–1174, Jun. 2011.
- [6] M. Miki, B. Felder, K. Tsuzuki, Y. Xu, Z. Deng, M. Izumi, H. Hayakawa, M. Morita, and H. Teshima, "Materials processing and machine applications of bulk HTS," *Superconductor Science and Technology*, vol. 23, no. 12, p. 124001, 2010.
- [7] D. Zhou, M. Izumi, M. Miki, B. Felder, T. Ida, and M. Kitano, "An overview of rotating machine systems with high-temperature bulk superconductors," *Superconductor Science and Technology*, vol. 25, no. 10, p. 103001, 2012.
- [8] C. P. Bean, "Magnetization of High-Field Superconductors," *Reviews of Modern Physics*, vol. 36, no. 1, pp. 31–39, 1964.
- [9] D.-X. Chen, D.-X. Chen, A. Sanchez, C. Navau, Y.-H. Shi, and D. A. Cardwell, "Critical-current density of melt-grown single-grain YBaCuO disks determined by ac susceptibility measurements," *Superconductor Science and Technology*, vol. 21, no. 8, p. 085013, 2008.
- [10] B. Douine, F. Sirois, J. Leveque, K. Berger, C. Bonnard, T. Hoang, and S. Mezani, "A New Direct Magnetic Method for Determining  $J_c$  in Bulk Superconductors From Magnetic Field Diffusion Measurements," *IEEE Transactions on Applied Superconductivity*, vol. 22, no. 3, p. 9001604, 2012.
- [11] B. Douine, C.-H. Bonnard, F. Sirois, K. Berger, A. Kameni, and J. Leveque, "Determination of  $J_c$  and  $n$ -Value of HTS Pellets by Measurement and Simulation of Magnetic Field Penetration," *IEEE Transactions on Applied Superconductivity*, vol. 25, no. 4, pp. 1–8, 2015.
- [12] M. D. Ainslie, M. D. Ainslie, and H. Fujishiro, "Modelling of bulk superconductor magnetization," *Superconductor Science and Technology*, vol. 28, no. 5, p. 053002, 2015.
- [13] I. Mayergoyz, "Chapter 4 - Nonlinear Diffusion in Superconductors," in *Nonlinear Diffusion of Electromagnetic Fields*, San Diego: Academic Press, 1998, pp. 225–303.
- [14] K. Berger, J. Leveque, D. Netter, B. Douine, and A. Rezzoug, "Influence of Temperature and/or Field Dependences of the E-J Power Law on Trapped Magnetic Field in Bulk YBaCuO," *IEEE Transactions on Applied Superconductivity*, vol. 17, no. 2, pp. 3028–3031, Jun. 2007.
- [15] A. Kameni, D. Netter, S. Mezani, B. Douine, and J. Leveque, "Scaling Solution and  $n$  Dependence of the Eddy-Current Distribution in a Flat Superconductor," *IEEE Transactions on Applied Superconductivity*, vol. 20, no. 4, pp. 2248–2254, 2010.
- [16] A. K. Kameni, J. Leveque, B. Douine, S. Mezani, and D. Netter, "Influence of Speed Variation of a Transverse Magnetic Field on a Magnetization of HTS Cylinder," *IEEE Transactions on Applied Superconductivity*, vol. 21, no. 4, pp. 3434–3441, 2011.
- [17] D.-X. Chen and E. Pardo, "Power-law  $E(J)$  characteristic converted from field-amplitude and frequency dependent ac susceptibility in superconductors," *Applied Physics Letters*, vol. 88, no. 22, p. 222505, 2006.
- [18] H. Yamasaki and Y. Mawatari, "Current-voltage characteristics and flux creep in melt-textured YBa<sub>2</sub>Cu<sub>3</sub>O<sub>7</sub>-delta," *Superconductor Science and Technology*, vol. 13, no. 2, pp. 202–208, 2000.
- [19] P. Vanderbemden, Z. Hong, T. A. Coombs, S. Denis, M. Ausloos, J. Schwartz, I. B. Rutel, N. H. Babu, D. A. Cardwell, and A. M. Campbell, "Behavior of bulk high-temperature superconductors of finite thickness subjected to crossed magnetic fields: Experiment and model," *Physical Review B*, vol. 75, no. 17, 2007.
- [20] M. P. Philippe, M. D. Ainslie, L. W era, J.-F. Fagnard, A. R. Dennis, Y.-H. Shi, D. A. Cardwell, B. Vanderheyden, and P. Vanderbemden, "Influence of soft ferromagnetic sections on the magnetic flux density profile of a large grain, bulk YBaCuO superconductor," *Superconductor Science and Technology*, vol. 28, no. 9, p. 095008, 2015.